



Design of Robust FOPI-FOPD Controller for Maglev System Using Particle Swarm Optimization

Salwan Y. Yousif^{a*}, Mohamed J. Mohamed ^{b*}

^a Control and Systems Engineering Department, University of Technology-Iraq, Baghdad, Iraq,
Babylon.telecom@gmail.com

^b Control and Systems Engineering Department, University of Technology, Baghdad, Iraq,
60098@uotechnology.edu.iq

* Corresponding author.

Submitted: 21/12/2020

Accepted: 30/01/2021

Published: 25/04/2021

KEY WORDS

Magnetic Levitation System, Robust Control, PID Controller, Fractional Order PID Controller, Particle Swarm Optimization (PSO).

ABSTRACT

Magnetic Levitation System (MLS) is one of the benchmark laboratories models for designing and testing feedback control systems in the presence of the parametric uncertainties and disturbances effect. Therefore, the MLS can be regarded as a tool to study and verify a certain robust controller design. In this paper, two types of powerful control schemes are presented to control the MLS. The first controller is a robust PI-PD controller, while the other is a robust fractional order FOPI-FOPD controller which provides two extra degrees of freedom to the system. In both controller design procedures, the Particle Swarm Optimization (PSO) algorithm is used to find the best values of controller parameters subject to the time-domain objective function and H_∞ constraints. All modeling processes including parameterization, optimization, and validation of the controllers are performed using MATLAB. The simulation results show that the MLS with robust FOPI-FOPD is faster and more stable than the MLS with robust classical PI-PD. Also, the proposed FOPI-FOPD controller gives far superior results than the PI-PD controller for disturbance rejection.

How to cite this article: S. Y. Yousif and M. J. Mohamed, "Design of Robust FOPI-FOPD Controller for Maglev System Using Particle Swarm Optimization," Engineering and Technology Journal, Vol. 39, Part A, No. 04, pp. 653-667, 2021.
DOI: <https://doi.org/10.30684/etj.v39i4A.1956>

This is an open access article under the CC BY 4.0 license <http://creativecommons.org/licenses/by/4.0>

1. INTRODUCTION

The PID controller is widely used in control design for simple and complex industrial systems for more than 60 years ago. The problem of using a PID controller is this controller sometimes hardly satisfies the requirements of good robustness by using three gain parameters K_p , K_i , and K_d . Therefore, Fractional Order PID (FOPID) controller is considered as a new version of the PID controller is used. The FOPID controller is the same as the PID controller in

gains but has an extra degree in the derivative and integral order. This degree is non-integer and can be adjusted from 0 to 2 [1]. Most real systems are especially exposed to measurement noise, external disturbance, and model uncertainty [2]. Therefore, robustness is an essential principle in controller design. On the other side, the classical controller does not guarantee to satisfy the robustness. So, a recent control theory aims to design a simple controller with a fixed order to satisfy multiple objectives (frequency-domain performance, Time-domain performance, and robust performance criterion). These controllers provide the same result as the standard H_∞ control design [3]. It is worth mentioning the robust fractional order controllers have better performance and robustness than conventional controllers because of the extra degree of freedom related to the order. The Magnetic Levitation System (MLS) is considered a good benchmark laboratory model for understanding control systems because it is a highly nonlinear and open-loop unstable system, as well as its internal dynamics, which are very complex. So, controlling such a system is a challenging task. Several control approaches were used to stabilize the MLS, such as fractional order PID controller [4,], PID controller [5], H_∞ controller [3, 6], fuzzy logic controller (FLC) [7], sliding mode controller (SMC) [8, 9]. This paper proposes PI-PD and FOPI-FOPD to stabilize the MLS and achieve adequate performance in presence of noise signals, disturbance, unmodeled system dynamics, and system parameters uncertainty [3]. The essential objective of the design is tuning the parameters of PI-PD and FOPI-FOPD controllers to achieve robustness. The result of robust PI-PD controller is compared with robust FOPI-FOPD to show the effect of the extra degree of FOPI-FOPD on robustness and time response of the controlled system. The particle swarm optimization PSO algorithm is used to obtain the best and optimal parameter values of the PI-PD and FOPI-FOPD controllers and the performance weighting function parameters, with a guarantee to a controlled system with robust stability and robust performance.

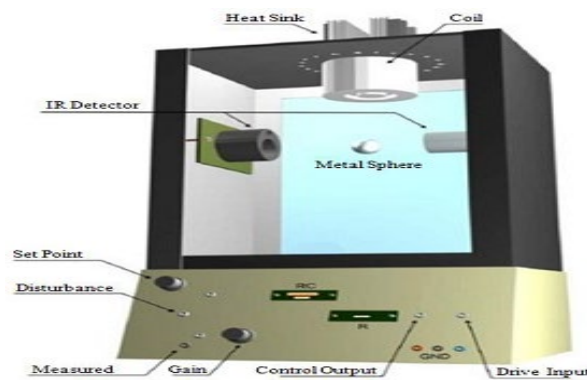


Figure 1: Electromagnetic levitation system [3].

2. MAGNETIC LEVITATION SYSTEM MODEL

The magnetic levitation system is shown in Figure 1 [3]. The system consists of an interface connection panel connected with the main electrical-mechanical part. The magnetic field is provided by electromagnetic coils mounted on the mechanical part. When the current is passed through the coil, the necessary lifting force is produced. This force directly impacts the metallic object. The temperature of the coil is regulating by the heat sink. In MLS, the infrared light (IR) sensor is used with a mechanical subsystem and consists of two parts transmitter and receiver, which incessantly measures the ball position by changing the ball's position to the initial ball position. The system MLS also contains an Analogue and Digital (A/D) interface, which is used to connect with a computer. This interface board is used to transfer the signal measured from the MLS system to the PC and the control signal from the PC to the MLS system. The electromagnetic levitation system is highly nonlinear, and the system open loop is unstable. Besides, to adjust the current through the coil, a suitable controller must be designed to stabilize the vertical position of the levitating ball and make it follow a reference trajectory. Deriving an exact model for the system is the first and important step in the control system from fundamental physics. Each element can be obtained from the behaviors of the system. Many equations are dependent on geometry and materials in the MLS system and are thus specific to the hardware. The free body diagram of MLS is shown in Figure 2 [3][10]

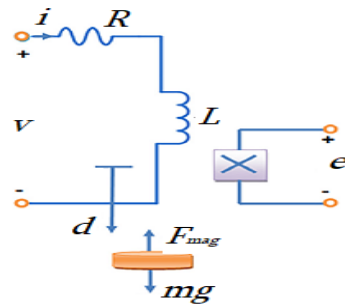


Figure 2: Electromagnetic levitation system free body diagram.

where: R and L is the resistance and inductance of the coil respectively.

i is the electric current passing in the electromagnetic circuit v is the voltage that is applied to the circuit g is the gravitational acceleration m is the mass of the levitating ball, d is the vertical distance from the bottom of the coil to the levitating ball, e is the voltage measured through the sensor, f is the magnetic force produced by the electromagnet As shown in Figure 2, two forces affect the ball, the gravity and electromagnetic force generated by the coils. The non-linear model is derived by analyzing electromagnetic and mechanical subsystems. So, after neglecting drag force and friction, Newton's 2nd law of motion is applied and given by [11, 12]:

$$f_{net} = f_g - f_{em} \tag{1}$$

$$m\ddot{x} = mg - c \frac{i^2}{x^2} \tag{2}$$

Where $f_{em} = c \frac{i^2}{x^2}$ and c is a constant depending on the coil (electromagnet) parameters, i is the current in the coil of the electromagnet, and x is the ball's position. f_{em} denotes the magnetic force generated by the coil. The electromagnetic force becomes equal to the gravitational force on the object at an equilibrium situation, the acceleration of the object is zero. So, Eq. (2) will be:

$$mg = c \frac{i^2}{x^2} \tag{3}$$

On the other hand, the electromagnetic part of the system is shown in Figure 2. By applying Kirchhoff's voltage and current laws, the following equations are developed:

$$e(t) = V_R + V_L = iR + L \frac{di}{dt} \tag{4}$$

Where:

$e(t) = u(t)$: Applied voltage.

V_R : Resistance voltage.

V_L : Inductance voltage.

The following differential equations express the nonlinear model of MLV based on the electro-mechanical mode [10]:

$$v = \frac{dx}{dt} \tag{5}$$

$$m\ddot{x} = mg - c \frac{i^2}{x^2} \tag{6}$$

$$u(t) = V_R + V_L \tag{7}$$

$$u(t) = iR + \frac{dL(x)i}{dt} \tag{8}$$

It's clear that from Eq. (8) that $L(x)$ is a non-linear function of balls position x . Different approaches are used for the determination of inductance for an MLS. In this work, we take the inductance changes with the inverse of the ball position, that is [10][11];

$$L(x) = L + \frac{L_0 x_0}{x} \quad (9)$$

Where L is the constant inductance of the electromagnetic coil without the suspended ball, x_0 is the equilibrium position, L_0 is the inductance caused by the effect of the ball. Substituting Eq. (9) into Eq. (8) results in [5];

$$u(t) = iR + \frac{d}{dt} \left(L_c + \frac{L_0 x_0}{x} \right) i \quad (10)$$

$$u(t) = iR + L \frac{di}{dt} - \left(\frac{L_0 x_0 i}{x^2} \right) \frac{dx}{dt} \quad (11)$$

Substituting $L_0 x_0 = 2c$, we get [11]

$$u(t) = iR + L \frac{di}{dt} - C \left(\frac{i}{x^2} \right) \frac{dx}{dt} \quad (12)$$

Using $x_1 = x$, $x_2 = V$ and $x_3 = i$ as the state of the system, $u = v_{in}$, the state equations that describe the system become [12]:

$$\frac{dx_1}{dt} = x_2 \quad (13)$$

$$\frac{dx_2}{dt} = g - \frac{c}{m} \left(\frac{x_3}{x_1} \right)^2 \quad (14)$$

$$\frac{dx_3}{dt} = -\frac{R}{L} x_3 + \frac{2c}{1} \left(\frac{x_2 x_3}{x_1^2} \right) + \frac{1}{L} u \quad (15)$$

The problem of nonlinearity can be solved by linearizing the nonlinear electromagnetic force. At the equilibrium state, the total model of the magnetic levitation system is obtained [3].

$$G(s) = \frac{x(s)}{u(s)} = \frac{-\left(\frac{2i_0}{x_0^2}\right)}{\frac{mL}{R}s^3 + ms^2 - c\left(\frac{2i_0^2}{x_0^3}\right)\frac{L}{R}s - c\left(\frac{2i_0^2}{x_0^3}\right)} \quad (16)$$

, where i_0 is the current in the coil of electromagnet at the equilibrium point, x_0 is the position of the ball at the equilibrium point, m is the metal sphere mass and g is the gravitational force. After substituting the values of m, g and x_0 in Eq. (3), c will equal to $6.53 \cdot 10^{-5}$. The magnetic ball position will be influenced by the inductance of the electromagnet coil.

3. PARTICLE SWARM OPTIMIZATION (PSO)

The PSO algorithm is one of the best optimization approaches, with great ability compared to other optimization methods. The PSO was produced in 1995 by Dr. Eberhart and Dr. Kennedy. In the PSO algorithm, the potential solutions of the problem are named "particles", these particles are connected with the best solution through the target that they wanted to achieve so far. A swarm of particles is put into the problem space search (D-dimensional) and treated as points in this dimension. At first, each particle takes a random position and initial velocity equal to zero. These particles fly throughout the search space according to the flying experience and a specific formula where each particle adjusts its flying. The best previous position which provides the maximum fitness value is recorded and called p_{best} while g_{best} of the population is the best particle among all particles.

The particle velocity and position of the standard PSO can be updated by the flowing equations [13,14]:

$$V_i(j) = V_i(j-1) + C_1 \cdot rand1 [P_{best\ i} - x_i(j-1)] + C_2 \cdot rand2 [G_{best} - x_i(j-1)] \quad (17)$$

$$\begin{aligned}
 & i = 1, 2, \dots, N \\
 x_i(j) &= x_i(j-1) + V_i(j) \\
 & i = 1, 2, \dots, N
 \end{aligned} \tag{18}$$

Where, $x_i(j)$ is the position of the i th particle at (j) iterations, $V_i(j)$ is the velocity of the j th particle at (j) iterations, $rand1$ and $rand2$ are uniformly distributed random numbers in the range 0 to 1, C_1 and C_2 are acceleration constants, and N is the number of particles in swarm [15]. Inertia term W is added to reduce the speed because the particle velocities usually grow up very fast. Usually, the assumed value of W changes linearly from (0.9 - 0.4) as the iterative process progresses. The particles' speed in a swarm with the term of inertia, as giving as the following [14,15]:

$$\begin{aligned}
 V_i(j) &= WV_i(j-1) + C_1 \cdot rand1 [P_{best\ i} - x_i(j-1)] + C_2 \cdot rand2 [G_{best\ i} - x_i(j-1)] \\
 & i = 1, 2, \dots, N
 \end{aligned} \tag{19}$$

The inertia weight W was added to the velocity equation to dampen the velocities over time (or iterations).

4. ROBUST CONTROL SYSTEM DESIGN

A robust control system aims to design a controller that can operate on the real dynamic system despite the uncertainties in its mathematical model. A robust control ensures stability and performance for the system if and only if the following characteristics are satisfied;

1. Nominal Stability.
2. Nominal Performance.
3. Robust Stability.
4. Robust Performance.

The performance analysis is defined in the frequency domain in terms of sensitivity functions at system inputs and/or at system outputs. These functions are the sensitivity function $S(s)$ and the complementary sensitivity function $T(s)$, and they are defined by the following equations [16, 17].

$$S(s) = (1 + G_p(s)K(s))^{-1} \tag{20}$$

$$T(s) = G_p(s)K(s)(1 + G_p(s)K(s))^{-1} \tag{21}$$

Figure 3 shows the feedback control system for the perturbation model with disturbance $d_y(s)$ and sensor noises $\eta(s)$. It can be seen that Eqs. (20) and (21) yield also to the following identity.

$$S(s) + T(s) = 1 \tag{22}$$

Nominal Stability.

A system satisfied this condition if the closed-loop of the controlled system has internal stability.

Nominal Performance.

Nominal performance requires the plant to satisfy all the requirements for the specific model. The nominal performance condition is [16, 17].

$$|W_p S| < 1 \quad \forall \omega \tag{23}$$

$$|W_p| < \frac{1}{|S|} = |1 + GK| \quad \forall \omega \tag{24}$$

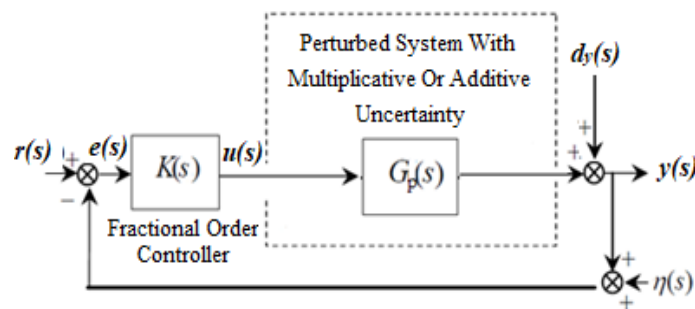


Figure 3: Feedback control model with disturbance $d_y(s)$ and sensor noises $\eta(s)$

Robust Stability.

The closed-loop system is robustly stable if the following condition is satisfied under the assumption of multiplicative uncertainty [16,18].

$$\|T(s)W_m(s)\|_\infty < 1 \tag{25}$$

While additive uncertainty is satisfied, if and only if the following condition is satisfied [16,18].

$$\|KS(s)W_a(s)\|_\infty < 1 \tag{26}$$

Robust Performance.

This condition requires robust stability as well as nominal performance [19].

1. Robust performance with multiplicative uncertainty condition:

$$\| |W_P(s)S(s)| + |T(s)W_m(s)| \|_\infty < 1 \tag{27}$$

2. Robust performance with additive uncertainty condition:

$$\| |W_P(s)S(j\omega)| + |KS(s)W_a(s)| \|_\infty < 1 \tag{28}$$

5. DESIGN METHODOLOGY OF THE WEIGHTING FUNCTION

A weighting function transfer function must be a stable minimum phase system. Some examples of the weighting functions are the performance weighting functions (W_P) and the uncertainty weighting function (W_m or W_a). All weighting functions add special constraints to the transfer function when multiplied by it.

Performance Weighting Functions (W_P)

The important part of the design of a robust controller is the selection of weighting function. This part is not an easy process and frequently needs more iterations of tuning. To select the performance weighting functions, the following general equations are used as first and second-order filters [18].

$$W_P^1(s) = \frac{s}{M_S + \omega_b} \tag{29}$$

$$W_P^2(s) = \frac{(\frac{s}{\sqrt{M_S}} + \omega_b)^2}{(s + \omega_b \sqrt{e_{SS}})^2} \tag{30}$$

ω_b : The minimum acceptable bandwidth (for disturbance rejection).

M_S : The maximum peak magnitude of $|S(j\omega)|$.

e_{SS} : Allowed steady-state error.

Note: $|S(s)| < \frac{1}{|W_P(s)|}$ the minimum of $\frac{1}{|W_P(s)|}$ is equal to e_{SS}

The parameters of the performance weighting function and the parameters of the controller are obtained using the PSO algorithm during minimizing the cost function.

Uncertainty Weighting Function

The design of robust control deals with both unstructured and structured uncertainty. However, the evaluation of the disk of uncertainty is done by selecting a set of nominal plants. The uncertainty weight function is used to bound all the uncertainty for the system.

The model with multiplicative uncertainty [20].

$$G_p(s) = G_n(s)(1 + w_m(s) \Delta_m) \quad (31)$$

where $\Delta_m \leq 1$.

From Eq. (31), the multiplicative uncertainty weight function $w_m(s)$ can be written as:

$$w_m(s) = \frac{G_p(s) - G_n(s)}{G_n(s)} \quad (32)$$

where,

$G_p(s)$: Transfer function of plant with uncertain parameter.

$G_n(s)$: Transfer function of plant with nominal parameter.

Thus, w_m represents the frequency response of all variations of plants' parameters. The curve fitting method is used to find uncertainty model by the following steps:

1. Plotting the frequency response of the system with all uncertain parameters.
2. Finding the largest magnitudes (upper bound frequency response) of the uncertain system.
3. Plotting a fitting curve that fits the plot of the large magnitude.
4. Selecting the curve order that fits the plot of the large magnitude.
5. The final uncertainty model (w_m) can be created after selecting a large curve's magnitudes with a suitable order.

In this work, the uncertainty model (w_m) is selected with the case of parameters uncertainty 10% as in Table I [21]. The determination of uncertainty weighting function $w_m(s)$ from the frequency responses of the family of the uncertain system is shown in Figure 4. The obtained uncertainty model is:

$$w_m(s) = \frac{0.17739s + 5.3}{s + 39.21} \quad (33)$$

TABLE I: The magnetic levitation nominal system parameters [21].

Parameter	Definition	Mini mum value	Value	Maxi mum Value	Unit
m	The mass of the ball	0.0612	0.068	0.0748	Kg
g	The gravitational constant		9.81		m/sec ²
R	The coil's resistance	9	10	11	Ω
L	The coil's inductance	0.3712	0.4125	0.4537	H
c	The magnetic force constant		$6.53 * 10^{-5}$		H/m
X₀₁	Initial position		0.012		Meter
X₀₂	Initial velocity		0		M/s
X₀₃	Initial current		0.5		Amp

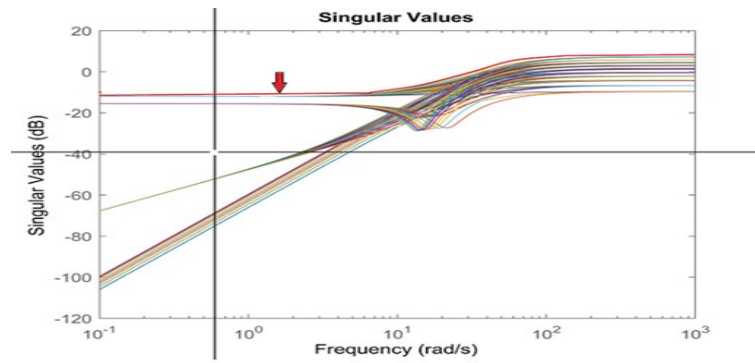


Figure 4: Determination of uncertainty weighting function $w_m(s)$ from the frequency responses of the family of uncertain system

6. COST FUNCTION

The optimal values of the controller parameters depending directly on the selected performance index. A performance index must be a positive number or zero. There are different types of performance criteria. The commonly used performance indices are [22]:

- Integral of Squared Error (ISE):

$$ISE = \int_0^\infty e^2(t)dt \tag{34}$$

- Integral of Time multiplied Squared Error (ITSE):

$$ITSE = \int_0^\infty te^2(t)dt \tag{35}$$

- Integral of Absolute Error (IAE):

$$IAE = \int_0^\infty |e(t)|dt \tag{36}$$

- Integral of Time multiplied Absolute Error (ITAE):

$$ITAE = \int_0^\infty t|e(t)|dt \tag{37}$$

, where, $e(t)$ is the error between the reference input and the output response.

In this paper, the PSO algorithm is used to optimize the cost function which is a combination of time-domain specifications represented by the performance index (ISE) and norm infinity specifications with multiplicative uncertainty. The cost function is:

$$\text{Cost Function} = \int_0^\infty |e(t)|dt + \|W_p S\|_\infty + \|W_m T\|_\infty \tag{38}$$

7. DESIGN AND IMPLEMENTATION OF ROBUST PI-PD CONTROLLER

In this section, the design of a robust PI-PD controller is introduced. The advantages of the robust PI-PD controller in the disturbance rejection and system parameters uncertainty can be verified. The block diagram of the system with PI-PD controller is shown in Figure 5. The transfer functions of PI and PD controllers are defined as [23]:

$$G(s) = \frac{N(s)}{D(s)} \tag{39}$$

$$PI(s) = K_p + \frac{K_i}{s} \tag{40}$$

$$PD(s) = K_G + K_d \frac{k_n}{1+k_n/s} \tag{41}$$

, where: $N(s)$ is the numerator of the system and $D(s)$ is the denominator of the system. (K_p, K_i) are the parameters of the outer loop controller portion PI while (K_G, K_d, k_n) are the parameters of inner loop controller portion PD. The PSO algorithm is used to obtain the best and optimal parameter values of the PI-PD controllers and the performance weighting function parameters with a guarantee to control the system with robust stability and robust performance. The step size of the simulation used in this case is $h_s = 0.001$ sec while the time of simulation is $T_{ob} = 100$ sec. The number of maximum iterations in the PSO is $I_{ter} = 5000$, Population Size = 10, inertia factor $h = 2$, $C_1 = C_2 = 2$. The cost function to be minimized using the PSO method is given in Equation (35).

The optimal parameters of the controller are shown in Table II and the parameters of the weighting performance function are:

$$W_p(s) = \frac{0.3546s + 0.701}{s + 1.81} \tag{42}$$

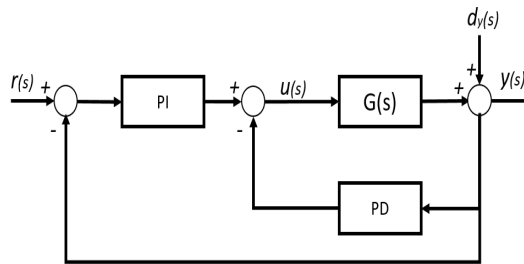


Figure 5: Block diagram of MLS with PI-PD controller

TABLE II: The optimal parameters of PI-PD controller and value of ISE criterion with robustness condition

Initial Position	K_p	K_i	K_G	K_d	k_n	$\ W_p S\ _\infty$	$\ W_m T\ _\infty$	ISE
0.012	146.9	86.506	965.45	113.56	0.002	0.4891	0.2233	0.0246

8. DESIGN AND IMPLEMENTATION OF ROBUST FOPI-FOPD CONTROLLER

This section introduces the design of a robust FOPI-FOPD controller for MLS to achieve robust stability and performance to control the position of the metal ball in a specific position. Now, consider the control system, as shown in Figure (6), where $G(s)$ is the actual plant that has some uncertainty, $K(s)$ is the FOPI-FOPD controller as shown in the following model, $r(t)$ is the reference input, $u(t)$ is the control input, $e(t)$ is the error signal, $d(t)$ is the external disturbance, and $y(t)$ is the system output response. In the modified structure of the FOPI-FOPD control, the FOPD control is used in the inner loop while the FOPI control is used in the outer loop. The components of the FOPD and FOPI control parts are defined as follows [23, 24, 25]:

$$G(s) = \frac{N(s)}{D(s)} \tag{43}$$

$$FOPI(s) = K_p + \frac{K_i}{s^\lambda} \tag{44}$$

$$FOPD(s) = K_G + K_d \frac{k_n}{1 + k_n/s^\delta} \tag{45}$$

, where: $N(s)$ is the numerator of the system and $D(s)$ is the denominator of the system. $FOPI$ is the outer-loop portion of the controller and the $FOPD$ is the inner loop portion of the controller. The FOPI-FOPD controller provides more flexibility and robustness in tuning while adding two extra

degrees of freedom to the system. These degrees of freedom are related to the orders of the integral and derivative parts (λ, δ) which are extended to non-integer (fractional) values [23, 24].

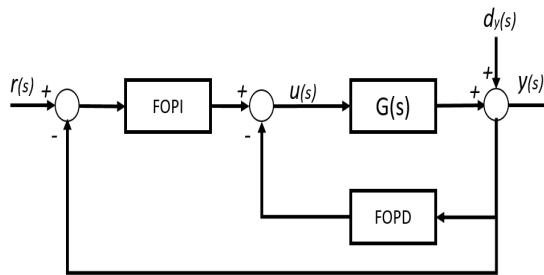


Figure 6: Block diagram of MLS with FOPI-FOPD controller.

The proposed FOPI-FOPD controller has an advantage where the internal FOPD controller is utilized to adjust the poles of the plant transfer function $G(s)$ to more suitable locations. Therefore, the FOPI-FOPD structure has extra more advantages over the conventional design FOPID controller [23]. The FOPI-FOPD is proposed to control integrating processes either with dead time or without dead time and processes with unstable transfer functions. The objective is to design the controller $K(s)$ or FOPI-FOPD to achieve the robustness conditions mentioned in section (4).

The PSO algorithm is used to obtain the best and optimal values of the FOPI-FOPD controller parameters and the performance weighting function parameters, as shown in Figure 7, with a guarantee to control the system with robust stability and robust performance. The step size of the simulation used in this case is $h_s = 0.001$ sec while the time of simulation is $T_{ob}=100$ sec. The number of maximum iterations in the PSO is $I_{ter}=5000$, Population Size=10, inertia factor $h = 2, C_1 = C_2 = 2$. The cost function to be minimized using the PSO method is given in Eq. (35).

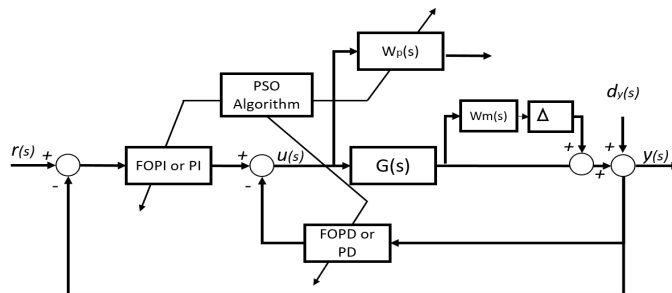


Figure 7: Block diagram of the proposed controller using PSO

The optimal parameters of the FOPI-FOPD controller are shown in Table III and the parameters of the weighting performance function are:

$$W_p(s) = \frac{0.446s+0.501}{s+1.01} \tag{46}$$

TABLE III: The optimal parameters of FOPID controller and the value of ISE criterion with robustness condition.

Initial Position	K_P	K_i	λ	K_G	K_d	k_n	δ	$\ W_p S\ _\infty$	$\ W_m T\ _\infty$	ISE
0.012	335.	989.	1.	883	117.	0.02	0.	0.5080	0.2421	0.0
	1	93	13	.2	36	58	95			16
							1			

9. RESULTS AND DISCUSSION

The MLS is a non-linear system moreover the system open-loop is highly unstable. Figure 8 and Figure 9 show the position responses of the linear and nonlinear systems respectively, where the initial conditions in this simulation are taken as established in Table I [23]. In both figures, the ball position curve goes to infinity, which describes that the ball is unsettled. Extensive tests on the magnetic levitation system have been performed to demonstrate the effectiveness of the proposed robust PI-PD and robust FOPI-FOPD controllers. From Figures 10 to 13, it can be seen that the magnitudes of sensitivity and complementary sensitivity functions are less than the magnitudes of the inverse of performance and uncertainty weighting functions for all frequencies and both robust PI-PD and robust FOPI-FOPD controllers. This means that robust stability and robust performance conditions in Eqs. (23) and (25) have been achieved. On the other hand, the obtained time response specifications for robust PI-PD and robust FOPI-FOPD controllers can be shown in Figure 14. Also, Table IV depicts the time response specifications for both robust controllers. The system with a robust FOPI-FOPD has less overshoot, less rise time, and less settling time than the same system with a robust classical PI-PD. That means the system is faster and more stable with a robust FOPI-FOPD controller than the system with robust classical PI-PD. On the other hand, to show the robustness of the proposed PI-PD controller and FOPI-FOPD controller, the disturbance (d) with the magnitude of 0.001 was added into the system at time 5.4 sec to 8.2 sec. The proposed FOPI-FOPD controller gives far superior results than the PI-PD controller for the setpoint response and excellent disturbance rejection. Figures 15 and 16 show the effect of disturbance on the control system. The step responses of the uncertain system as in Table I [21] with the robust PI-PD controller and robust FOPI-FOPD controller are shown in Figures (17) and (18) respectively. Furthermore, the time response specifications of the control efforts using the robust PI-PD controller and robust FOPI-FOPD controller are shown in Figure 19 and Figure 20, respectively.

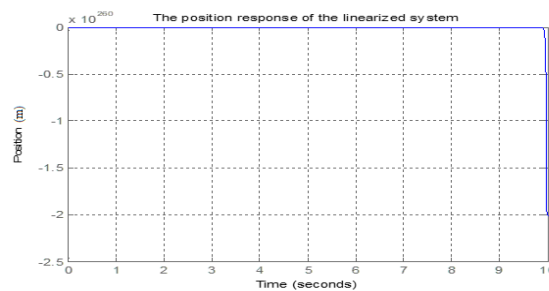


Figure 8: The unstable ball position response for linear model

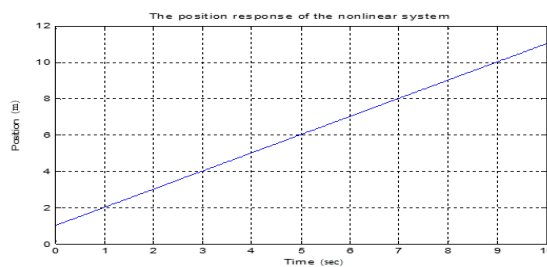


Figure 9: The unstable ball position response for nonlinear model

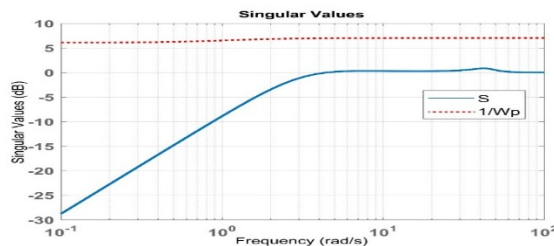


Figure 10: The Frequency characteristics of sensitivity function S using the robust PI-PD controller and the inverse of the weighting function W_p

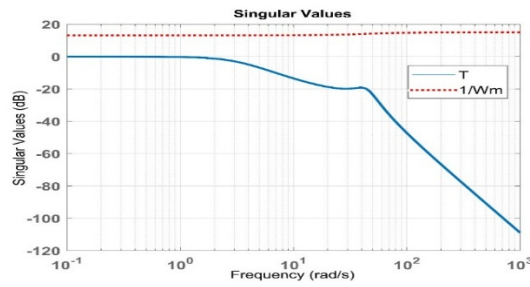


Figure 11: The Frequency characteristics of complementary sensitivity function T using the robust PI-PD controller and the inverse of the weighting function W_m .

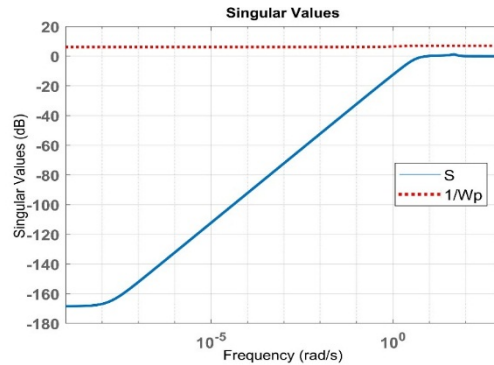


Figure 12: The Frequency characteristics of sensitivity function S using the robust FOPI-FOPD controller and the inverse of the weighting function W_p .

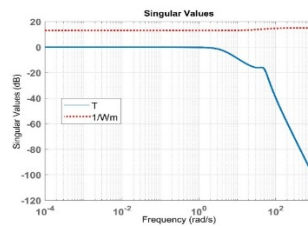


Figure 13: The characteristics of complementary sensitivity function T using the robust FOPI-FOPD controller and the inverse of the weighting function W_m .

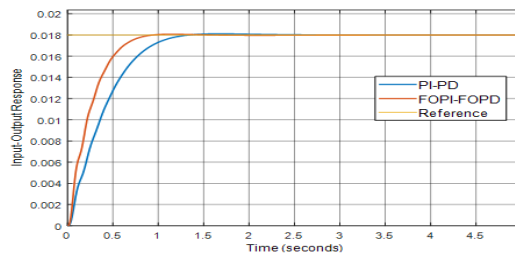


Figure 14: The position of the ball of MLS with PI-PD and FOPI-FOPD controllers.

TABLE IV: The time response specifications for both controllers

Transient Parameter	Robust FOPI-FOPD	Robust PI-PD
Rise Time (T_r)	472.277ms	727.756ms
Settling Time (T_s) 5%	0.7499 s	1.0634s
Peak time (T_p)	2.6192 s	1.5906
Overshoot (M_p)	0.3103%	0.689%

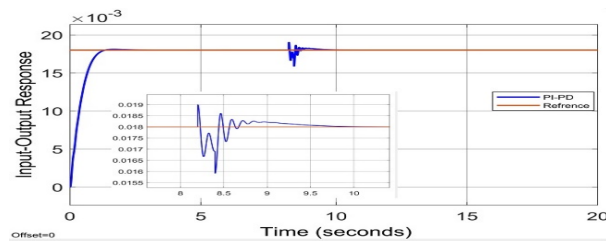


Figure 15: Setpoint and disturbance responses for PI-PD controlled system

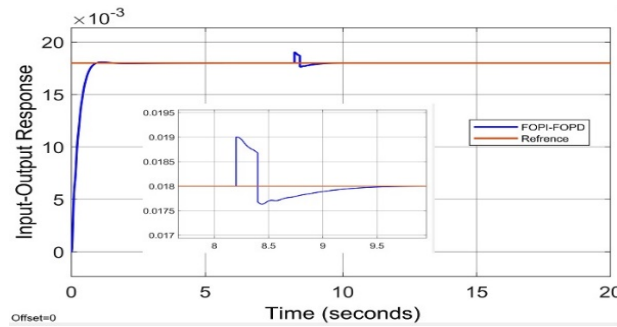


Figure 16: Setpoint and disturbance responses for FOPI-FOPD controlled system

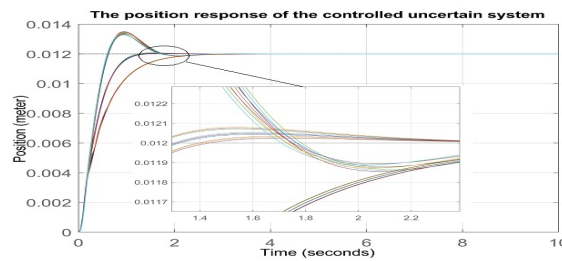


Figure 17: Figure (17): The close loop response when PI-PD controller is used with 10% parameter uncertainty

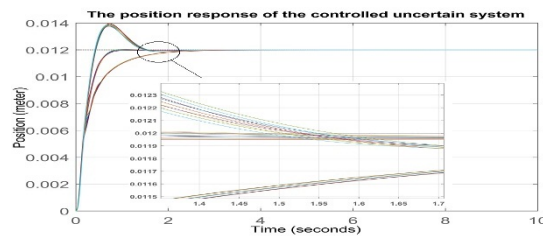


Figure 18: The close loop response when FOPI-FOPD controller is used with 10% parameter uncertainty

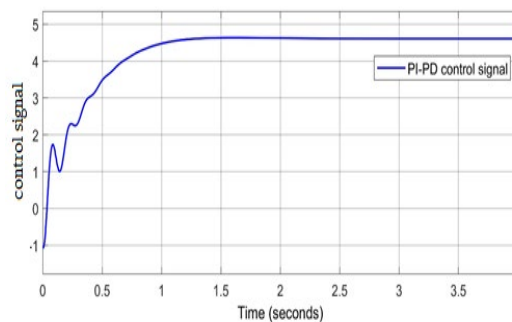


Figure 19: The resultant control signal for the designed robust PI-PD controller.

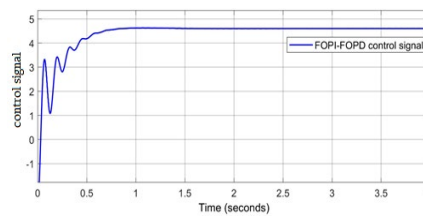


Figure 20: The resultant control signal for the designed robust FOPI-FOPD controller.

10. CONCLUSION

In this paper, a robust FOPI-FOPD controller has been presented as a new version of robust PI-PD because it has an extra fractional order in the derivative and integral. The particle swarm optimization (PSO) algorithm was used to find both the optimal parameters of the robust controller and the optimal parameters of the performance weighting function for each controller. The proposed controllers have been applied to MLS which is considered as one of the high nonlinearities and uncertain systems. The unstructured multiplicative uncertainty was used to express the uncertainty of MLS. The robust performance and stability of the system have been achieved with both PI-PD and FOPI-FOPD controllers. The robust PI-PD and FOPI-FOPD controllers have achieved adequate frequency and time response specifications. The results showed the superiority of the proposed FOPI-FOPD controller by provides more flexibility and robustness in tuning because of adding two extra degrees of freedom, On the other hand, the system with a robust FOPI-FOPD has less overshoot, less rise time, and less settling time than the same system with a robust classical PI-PD. That means the system is faster and more stable with a robust FOPI-FOPD controller than the system with robust classical PI-PD. The proposed FOPI-FOPD controller gives far superior results than the PI-PD controller for disturbance rejection.

References

- [1] I.Podlubny, Fractional-order systems and PI_D_ controllers, IEEE Trans. Automat. Contr., 44 (1999) 208-214. <http://dx.doi.org/10.1109/9.739144>
- [2] M. Hedayati , N. Mariun , M. Hojabri , Design of robust controller for statcom applied to large induction motor using graphical loop shaping method, J. Electr. Eng. J., 2012.
- [3] H. I. ALI, M. I. Abd, Optimal Multi-objective Robust Controller Design for Magnetic Levitation System, Iraqi J. Comp. Comm. Cont. Sys. Eng., 15 (2015) 18-34.
- [4] S. Folea , Theoretical analysis and experimental validation of a simplified fractional order controller for a magnetic levitation system, IEEE Trans. Control. Syst. Technol., 24 (2016) 756-763. <http://dx.doi.org/10.1109/TCST.2015.2446496>
- [5] S. K. Choudhary, Robust feedback control analysis of magnetic levitation system, WSEAS Trans. Syst., 13 (2014) 285-291. <http://dx.doi.org/10.5281/zenodo.2590932>
- [6] T. Salim , V. M. Karsli, Control of single axis magnetic levitation system using fuzzy logic control, Int. J. Adv. Comput. Sci. Appl., 4 (2013) 83-88. <http://dx.doi.org/10.14569/IJACSA.2013.041111>
- [7] E. T. Moghaddam , J. Ganji, Sliding mode control of magnetic levitation systems using hybrid extended Kalman filter, Energy. Sci. Technol., 2 (2011) 35-42. <http://dx.doi.org/10.3968/j.est.1923847920110202.114>
- [8] S. A. Al-Samarräie, Variable Structure Control Design for a Magnetic Levitation System, J. Eng., 24 (2018) 84-103.
- [9] S. A. Al-Samarräie, Adaptive sliding mode control for magnetic levitation system, Al-Nahrain J. Eng. Sci., 21(2018) 266-74. <https://doi.org/10.29194/NJES21020266>

- [10] Zeltom LLC Electromagnetic Levitation System User Manual, release 1.3, March17, 2011.
- [11] S. A. Singh, Magnetic Levitation Methods and Modeling in Maglev Trains , Int. J. Advan. Res. Comp. Sci. Soft. Eng. , 4 (2014).
- [12] I. Ahmad, M. A. Javaid , Nonlinear Model & Controller Design for Magnetic Levitation System, recent Adv. SIG. Proc. Robot. Autom., 1790-5117.
- [13] M. J. Mohamed , A. Khashan, Comparison Between PID and FOPID Controllers Based on Particle Swarm Optimization, The Second Eng. Conf. Control. Comp. Mechatron. Eng., (2014).
- [14] M. E. El-Telbany, Employing particle swarm optimizer and genetic algorithms for optimal tuning of PID controllers: A comparative study, ICGST-ACSE J., 7 (2007) 49-54.
- [15] A. A. El-Saleh, M. Ismail, R. Viknesh, C. C. Mark, M. L. Chen, Particle swarm optimization for mobile network design, IEICE Electron. Expr., 6 (2009) 1219-1225. <https://doi.org/10.1587/elex.6.1219>
- [16] J. Zhang, L. He, E. Wang , R. Gao, Robust Active Vibration Control of Flexible Structures Based on H/spl infinity/ Control Theorem, Int. Workshop., 978 (2009) 4244-3894. <https://doi.org/10.1109/IWISA.2009.5073101>
- [17] J. S. Kim, J. H. Kim, J. M. Park, S. M. Park, W. Y. Choe , H. Heo, Auto Tuning PID Controller based on Improved Genetic Algorithm for Reverse Osmosis Plant, World. acad. Sci. eng. technol., 2 (2008).
- [18] A. Sarjaš, Solution of a mixed sensitivity problem with optimized weights and time performance index for a robust servo velocity and position controller, J. Prz. Elektrotech., 89 (2013).
- [19] A. AbdIrahem, H. Albalawi, A Multi-Model Approach to Design a Robust SVC Damping Controller Using Convex Optimization Technique to Enhance the Damping of Inter-Area Oscillations Considering Time Delay, Energy . Power. Eng., 9 (2017) 750-771. <https://doi.org/10.4236/epe.2017.912047>
- [20] D. Richard, Modern Control System, Upper Saddle River, New Jersey: Prentice Hall Inc, 2001.
- [21] S. K. Choudhary, Robust Feedback Control Analysis of Magnetic Levitation System, J. Trans. Syst., 13 (2014) 285-291 . <https://doi.org/10.5281/zenodo.2590932>
- [22] R. C. Dorf, R. H. Bishop, Modern control systems, Pearson Education, Inc., (2008) 1024
- [23] M. Dulau, A. Grigor, T. M. Dulau, Fractional order controllers versus integer order controller, Proc. Eng., 181 (2017) 538-545. <https://doi.org/10.1016/j.proeng.2017.02.431>
- [24] Y. Chen, I. Petr'a's , D. Xue , Fractional Order Control - A Tutorial , Am. Control. Conf ., (2009) 10-12. <https://doi.org/10.1109/ACC.2009.5160719>
- [25] M. J. Mohamed , A. Khashan, Comparison Between PID and FOPID Controllers Based on Particle Swarm Optimization , Eng. Conf. Control. Comput . Geotech Eng., (2014).